Supplementary information

Self-releasing reactive oxygen species based on metal-to-MOF charge transfer effect boosts electrochemiluminescence

Xuena Mei, Shuang Zhou,* Jing Zhang,* Mei Yan, Jinghua Yu and Yan Zhang*

School of Chemistry and Chemical Engineering, University of Jinan, Jinan 250022, China
E-mail: jnzs2022@126.com; zhangjingdadi@126.com; chm_zhangyan@hotmail.com

1. Experimental Section

1.1 Reagents

2-methylimidazole, luminol, N,N-dimethylformamide (DMF), acetic acid, chitosan, 1,3-Diphenylisobenzofuran (DPBF), 4-nitro blue tetrazolium chloride (NBT), 3,3',5,5'-tetramethylbenzidin (TMB), N-hydroxy succinimide (NHS), and 1-(3-diaminopropyl)-3-ethylcarbodiimide hydrochloride (EDC) were purchased from Shanghai Macklin Biochemical Co., Ltd. (Shanghai, China). Potassium hexacyanoferrate (III) ($K_3[Fe(CN)_6]$), and potassium ferrocyanide (II) ($K_4Fe(CN)_6 \cdot 3H_2O$) were obtained from Damao chemical reagent factory (Tianjin, China). Tris-HCl buffer solution (1 M, pH 7.4) was used for preparation and hybridization of DNA stock solutions. Deionized water with an electrical resistivity of 18.25 MΩ·cm was used throughout the experiments. Streptavidin (SA), zinc power, L-cysteine, 2-Morpholinoethanesulfonic acid hydrate (MES), PBS containing 0.05% tween-20, and dopamine hydrochloride (DA) were gained from Aladdin Biochemical Technology Co., Ltd. (Shanghai, China). LbCas12a (Cpf1) and oligonucleotides used in this work were supplied by Sangon Biotech. Co., Ltd. (Shanghai, China) and the sequences were as follows (5'-3'):

Aptamer: GATCGGGTGTGGGTGGCGTAAAGGGAGCATCGGACA

active DNA (acDNA): ACTCCGATGCTCCCTTTACGCCACCCACACCTCGAT

crRNA: UAAUUUCUACUAAGUGUAGAUGUGGCGUAAAGGGAGCAUCG

ssDNA: COOH-CACTATAGGAAGAGAT-biotin

1.2 Apparatuses

Scanning electron microscopy (SEM) analyses were conducted on a ZEISS Gemini300 field emission scanning electron microscopy (ZEISS Co., Germany), and the microscope was equipped with an energy dispersive spectrometer (EDS, Oxford, Britain). High resolution transmission electron microscope (HRTEM) image was acquired using a JEM-2100F instrument (JEOL, Japan) to obtain the morphology of L-CDs. X-ray diffraction (XRD) patterns were collected on a D8 advanced diffractometer system equipped with Cu Kα radiation (Bruker Co., Germany). Infrared spectroscopy (IR) was recorded on a VERTEX 70 Fourier transform infrared (FT-IR) spectrometer. (Bruker Co., Germany). X-ray photoelectron spectroscopy (XPS) was performed on an ESCALAB MK II X-ray photoelectron spectrometer (Thermo Fisher Scientific Co., Britain). Mott-schottky (M-S) and electrochemical impedance spectra (EIS) assay was carried out using the VersaSTAT 3F Electrochemical Princeton Applied Research (AMETEK Co., United States). Time-resolved photoluminescence decay measurements were recorded on a FLS980 fluorescence spectrometer (Edinburgh Instruments,

Britain). The generation of reactive oxygen species was measured by electron spin resonance (ESR) (Bruker Co., Germany). Ultraviolet-visible (UV-vis) diffuse reflectance spectroscopy was obtained on a UV-2550 spectrophotometer (Shimadzu, Japan). All of electrochemiluminescence (ECL) measurements were conducted on an MPI-E ECL analyzer from (Xi'an Remex Electronic Science & Technology Co. Ltd., China) in 0.1 M pH 7.4 PBS containing 0.1 M KCl.

1.3 Preparation of Zn-MOF/L-CDs

Prior to experiment, Zn-MOF was synthesized via a straightforward solvothermal approach. In detail, zinc powder (9.9960 g) was mixed with 2-methylimidazole (0.5020 g) in a deionized water/DMF solvent mixture (20 mL, 1:2 in volume) with magnetic stirring and then heated at 80°C for 20 h (**Fig. 1A**). Zn-MOF was obtained after the mixture was cooled to room temperature. The powders were then washed with ethanol and allowed to dry at 60°C in an oven overnight.

L-CDs were synthesized by the traditional hydrothermal method.[1] Initially, 53.0 mg luminol and 36.0 mg L-cysteine (molar ratio 1:1) were dissolved in 20 mL acetic acid via ultrasonic dispersion. The resulting mixture was transferred into a Teflon-lined stainless steel autoclave (50 mL) and heated at 180°C for 10 h. After centrifuging three times at 10,000 rpm for 10 min each time to remove large particles, the sample was dialyzed with deionized water for 48 h using a 1000 Da dialysis membrane. Ultimately, the purified L-CDs were dried under vacuum conditions at 60°C for further use.

Zn-MOF/L-CDs were fabricated through a chitosan-mediated cross-linking protocol. 5.0 mg of chitosan was solubilized in 5 mL of aqueous acetic acid solution (2%, v/v) under continuous stirring. Then 5.0 mg of Zn-MOF was uniformly dispersed into the chitosan solution via ultrasonic treatment. Subsequently, 3.0 mg of L-CDs was introduced into the mixture. The reaction system was maintained under static incubation at ambient temperature for 12 h to facilitate interfacial interactions. Ultimately, the resultant Zn-MOF/L-CDs were isolated through centrifugation and redispersed in 5 mL of PBS (pH 7.4) and stored at 4°C for subsequent use.

As a comparison, Zn-MOF+L-CDs solution were fabricated through a simple mixing method. 5.0 mg of Zn-MOF and 3.0 mg of L-CDs was solubilized in 5 mL of aqueous solution.

The stable combination of L-CDs with Zn-MOF was promoted by the abundant amino and hydroxyl functional groups inherent to chitosan.[2] Simultaneously, chitosan was utilized to prevent the aggregation of Zn-MOF/L-CDs, thereby ensuring the composite uniform dispersion

on the electrode surface and enhancing the utilization efficiency of active sites. Based on this, chitosan was employed to improve thDe stability of the composite and its uniform loading on the electrode, ultimately leading to an increase in ECL intensity.

1.4 Preparation of ZnO

Initially, $Zn(CH_3COO)_2$ (0.7340 g, 4mmol) was dissolved in 40 mL of ethanol. This mixture was stirred continuously for 1 h. Subsequently, 40 mLof 0.1M KOH solution was added gradually, with continued stirring for an additional 6 h, resulting in a viscous precursor solution. This precursor was then transferred to a Teflon-lined autoclave and subjected to a temperature of 150 °C for 20h. Post-synthesis, the resultant material was thoroughlywashed thrice using deionized water and ethanol and subsequently dried at 60°C over 12 h.

1.5 Target-triggered trans-cleavage of CRISPR/Cas12a system

Initially, 5 μL of 0.1 μM OTA aptamer was hybridized with 5 μL of 0.1 μM acDNA to form double-stranded DNA (dsDNA). Next, 5 μL of OTA at different concentrations was added to the dsDNA, and different concentrations of acDNA were generated due to the specific recognition of OTA and the aptamer. After that, 15 μL of the mixture (including 100 nM Cas12a, 120 nM crRNA, and 1 × buffer) was incubated at 37°C for 10 min to obtain a Cas12a-crRNA solution. Next, 5 μL of acDNA at different concentrations was added to the pretreated Cas12a-crRNA and reacted at 37°C for 20 min to activate the CRISPR/Cas12a shearing system.

1.6 Synthesis of magnetic beads

A homogeneous precursor solution was prepared by dissolving anhydrous ferric chloride (0.6500 g) and trisodium citrate dihydrate (0.2000 g) in 20 mL of ethylene glycol under magnetic stirring. Subsequently, sodium acetate anhydrous (1.2020 g) was gradually introduced into the mixture, followed by continuous agitation at ambient temperature for 30 min. The resulting solution was transferred to a 50 mL Teflon-lined stainless steel autoclave and subjected to hydrothermal treatment at 200°C for 10 h. The black precipitate obtained was sequentially purified through three cycles of ethanol washing (10 mL × 3) via centrifugation (8,000 rpm, 10 min) and vacuum-dried at 60°C for 12 h to yield the final product. As exhibited in the SEM image of **Fig. S6**, the magnetic beads (MBs) exhibited uniform spheres.

1.7 Preparation of SA-modified MBs

The synthesized MBs (10 mg mL^{-1}, 200 μL) were sequentially washed with MES buffer (25 mM, pH 5.0). Carboxyl groups on the MBs were activated by incubating with 100 μL EDC (50 mg mL^{-1}) and 100 μL NHS (50 mg mL^{-1}) under gentle shaking (25°C, 30 min). After washing with MES buffer, the activated MBs were incubated with 200 μL MES containing 100 μg SA overnight (25°C) to immobilize SA. The resulting SA-modified MBs (SA-MBs) were washed three times with PBS (0.1 M, pH 7.4) and blocked with Tris-HCl buffer (20 mM Tris-HCl, 140 mM NaCl, 5 mM KCl, pH 7.5) for 12 h to passivate unreacted carboxyl groups via amide condensation. Finally, SA-MBs were washed with PBS containing 0.05% tween-20, resuspended in 200 μL PBS, and stored at 4°C.

1.8 Integration of DA-ssDNA modified SA-MBs

The DA-ssDNA probes were synthesized by first activating the terminal carboxyl groups of ssDNA (5 μM, 200 μL) through incubation with EDC (50 mg mL^{-1}, 100 μL) and NHS (50 mg mL^{-1}, 100 μL) under gentle agitation at 4°C for 2 h. DA (10 mM, 300 μL) was then added dropwise to the activated ssDNA solution, followed by overnight stirring at 25°C to covalently conjugate DA molecules. Subsequently, the DA-ssDNA (40 μL) was incubated with SA-MBs (10 mg mL^{-1}, 20 μL) for 1 h to immobilize the probes via biotin-streptavidin affinity. The resulting MBs-probe conjugates were thoroughly washed three times with PBS containing 0.05% tween-20 and stored in PBS for further use.

1.9 Fabrication of ECL sensing platform

Initially, 1% Nafion solution was applied to the glass carbon electrode (GCE) to enhance the stability of the electrode. 30 μL of Zn-MOF/L-CDs (the mass ratio of 5:3) was uniformly deposited onto the GCE and allowed to dry at room temperature atmosphere producing the ideal sensing platform. For target-triggered signal amplification, 2 μL of the MBs-probe was introduced into the CRISPR/Cas12a system, resulting in the generation of a substantial quantity of DA-ssDNA, facilitated by the exceptional trans-cleavage capability of Cas12a. Subsequently, the reaction mixture was subjected to magnetic separation, and the supernatant containing DA-ssDNA was collected. Ultimately, 20 μL of the supernatant was drop-coated onto the sensing platform for ECL measurement. ECL testing solution was consisted of 0.1 M PBS containing 0.1 M KCl (pH 7.4). ECL signals were recorded over a potential range from 0 to 0.8 V (vs. Ag/AgCl) was applied with the photomultiplier tube voltage maintained at 650 V.

2. Results and Discussion

2.1 DFT calculations

DFT calculations were performed using the Vienna Ab initio Software Package.[3] Perdew-Burke-Ernzerh is an exchange-related functional used to describe generalized gradient approximation. The projector augmented wave approach was also employed in electron-ion interactions and the DFT-D3 method was considered in all calculation procedures. A 20 Å vacuum layer was established vertically and the Monkhorst-Pack k-point was chosen as 1× 1 × 1 for during optimizing geometry and static energy calculations of the primitive cell. The cut-off energy of plane wave, total energy and force converge was set to 500 eV, 1×10^{-5} eV, and 0.01 eV/Å, respectively. Gibbs free energy (ΔG) of the intermediates was calculated to explore the reaction pathways of reactive oxygen species using the following equation:

$$\Delta G = \Delta E_{DFT} + \Delta E_{ZPE} - T\Delta S$$

where ΔE_{DFT} represents the energy change from DFT calculations, ΔE_{ZPE} is the zero-point energy correction, and ΔS denotes the entropy change of the reaction. T is the temperature and set to 298.15 K.

2.2 Optimization of the experimental conditions

In pursuit of maximizing the analytical capabilities of the ECL sensing platform, the optimization of three critical experimental parameters was undertaken, including the pH value of the PBS, the mass ratio of Zn-MOF to L-CDs, and the incubation time of OTA with aptamer/acDNA. As revealed in **Fig. S7A**, the pH-dependent ECL response was evaluated over a range from 6.5 to 8.5, exhibiting a parabolic trend with maximum intensity at pH 7.4. Consequently, pH 7.4 was selected as the optimal PBS condition to maximize sensitivity. Similarly, the effect of the Zn-MOF to L-CDs mass ratio varied from 5:1 to 5:5 was assessed (**Fig. S7B**). It was observable that the ECL intensity initially raised and subsequently declined as the mass ratio of Zn-MOF with L-CDs was progressively elevated, making 5:3 the optimal mass ratio for enhanced sensitivity. Under the optimal mass ratio of Zn-MOF with L-CDs, the impact of the incubation time for OTA with aptamer/acDNA was examined over a period ranging from 20 to 100 min (**Fig. S7C**). The ECL intensity gradually decreased over time, stabilizing at a plateau after 60 min. Consequently, an incubation time of 60 min for OTA with the aptamer/acDNA complex was selected as optimal for subsequent experiments.

2.3 DNA polyacrylamide gel electrophoresis

Buffer for DNA hybridization products were analyzed on a 20% polyacrylamide gel. 5 μL of the sample was mixed with DNA loading buffer and loaded. Firstly, the entropy-driven SDA-coupled electrophoresis was performed at 120 V for 120 min. It was then stained with Gel Red solution, shaken for 30 min, and imaged under UV light.

2.4 Pretreatment of real samples

Real sample analysis was conducted via standard addition using a validated extraction protocol.[4] Briefly, 2.0100 g of homogenized sample was mixed with 5 mL of acetonitrile/water/acetic acid (70:29:1, v/v) and shaken for 30 min to ensure OTA adequate dissolution. After centrifugation, 5 mL of supernatant was collected as the sample matrix. For the standard addition method, 5 mL of the supernatant was fortified with 0.5, 5, or 10 μL of OTA solution (1 μg mL^{-1}). Afterwards, 30 μL of the spiked solutions were analyzed using the ECL sensing platform under optimized conditions.

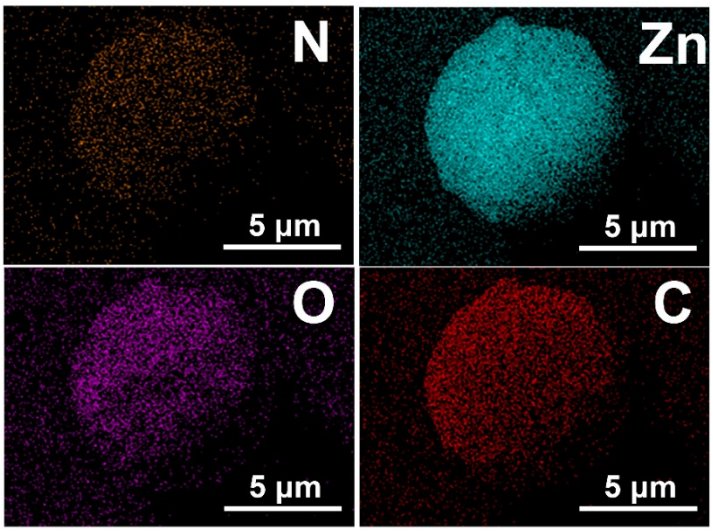

Fig. S1 SEM-EDS elemental mapping: N, Zn, O, C of Zn-MOF.

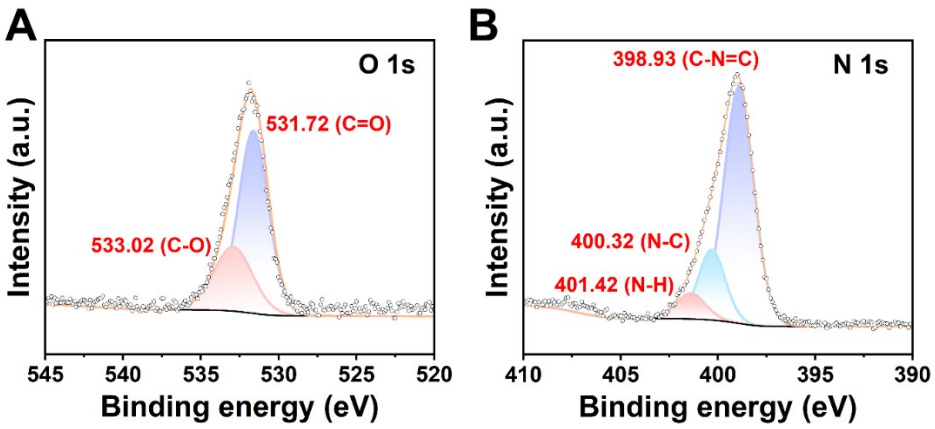

Fig. S2 XPS spectrum of (A) O 1s and (B) N 1s.

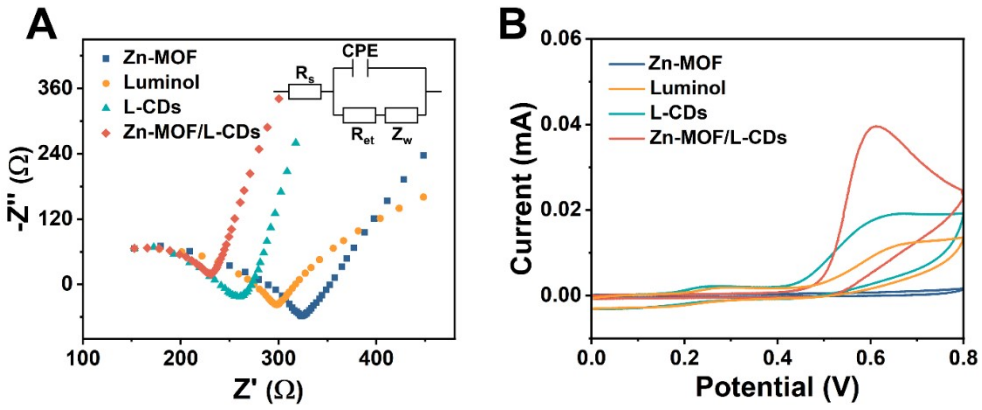

Fig. S3 (A) EIS of Zn-MOF, Luminol, L-CDs, and Zn-MOF/L-CDs modified GCE in 5 mM $[Fe(CN)_6]^{3-/4-}$ solution containing 0.1 M KCl. (B) Cyclic voltammetry of Zn-MOF, Luminol, L-CDs, and Zn-MOF/L-CDs modified GCE in 0.1 M PBS (pH 7.4).

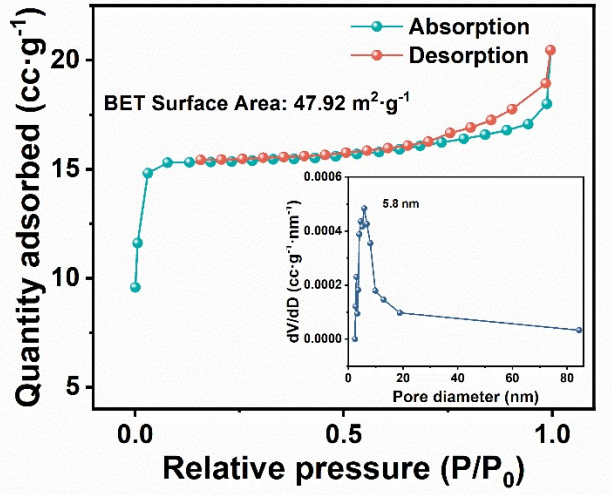

Fig. S4. BET surface area analysis and pore size distribution of Zn-MOF.

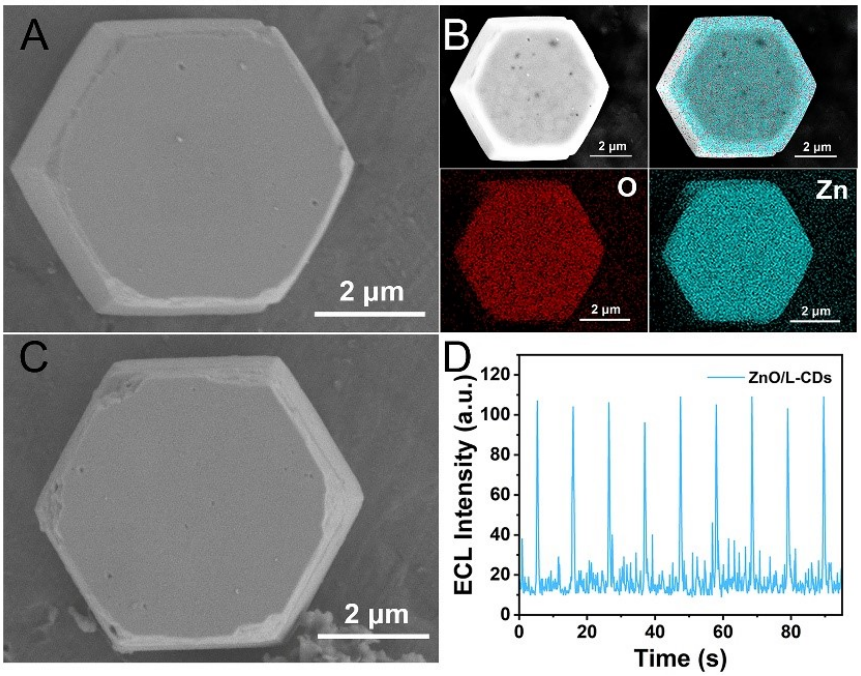

Fig. S5 (A) SEM image and (B) SEM-EDS elemental mapping of ZnO. (C) SEM image of ZnO/L-CDs. (D) ECL intensity of ZnO/L-CDs-modified electrodes in 0.1 M PBS (pH 7.4).

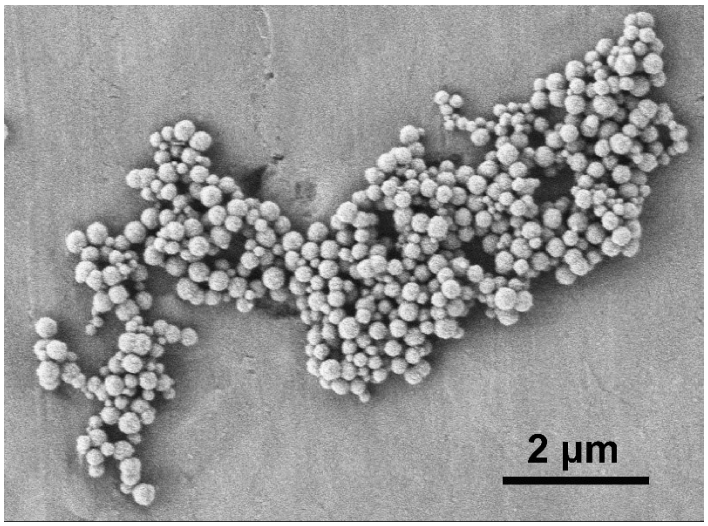

Fig. S6 SEM image of magnetic beads.

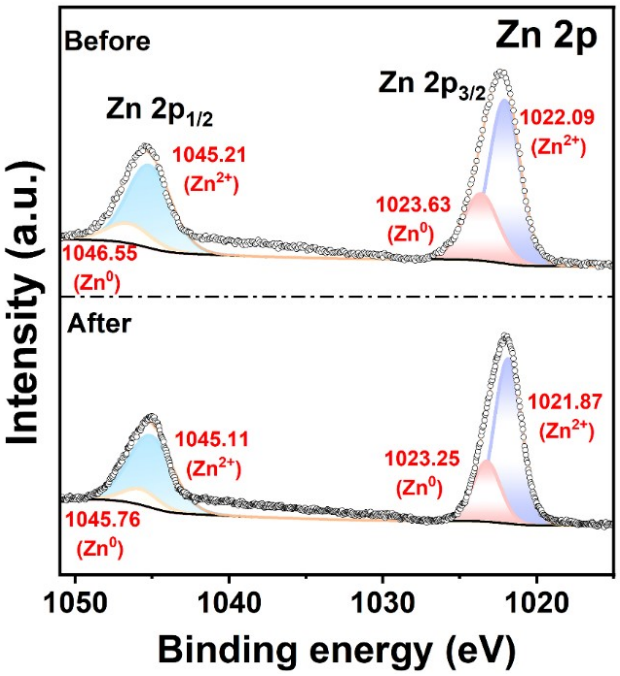

Fig. S7 Zn 2p XPS spectrum of Zn-MOF before and after ECL reaction.

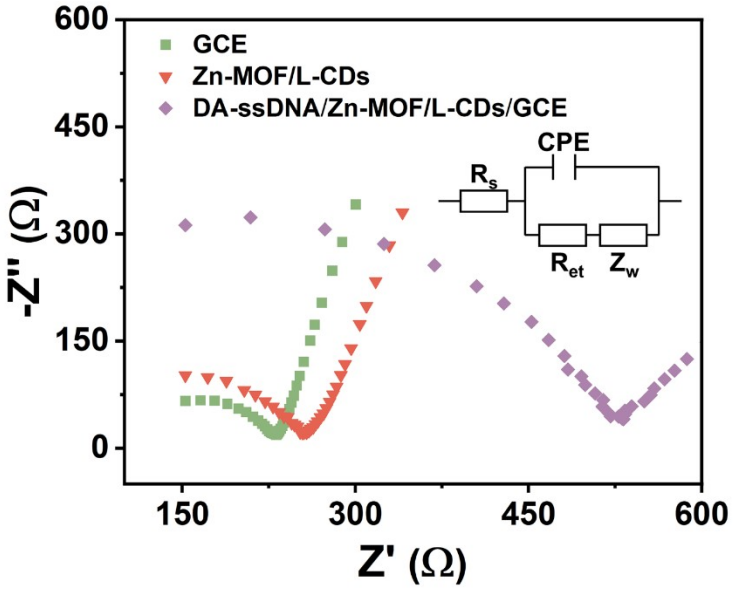

Fig. S8 EIS of bare GCE, Zn-MOF/L-CDs and DA-ssDNA modified GCE in 5 mM $[Fe(CN)_6]^{3-/4-}$ solution containing 0.1 M KCl.

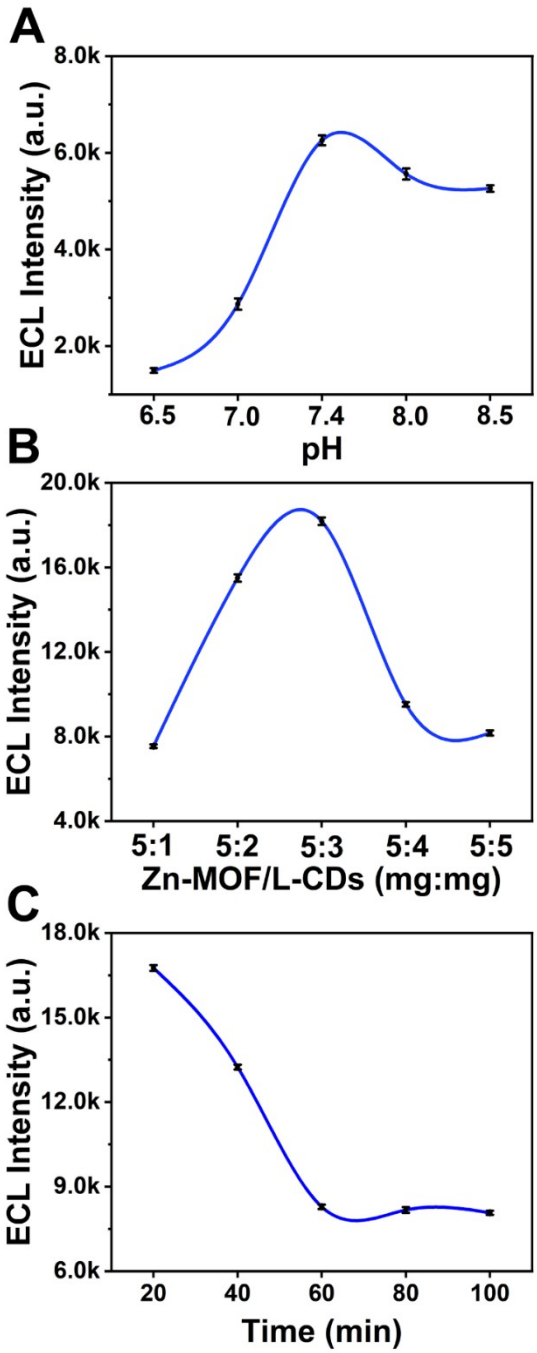

Fig. S9 Effects of (A) pH of PBS, (B) mass ratio of Zn-MOF with L-CDs and (C) incubation time of OTA with aptamer/acDNA on the ECL intensity. Error bars in all graphs represent standard deviations in triplicated experiments.

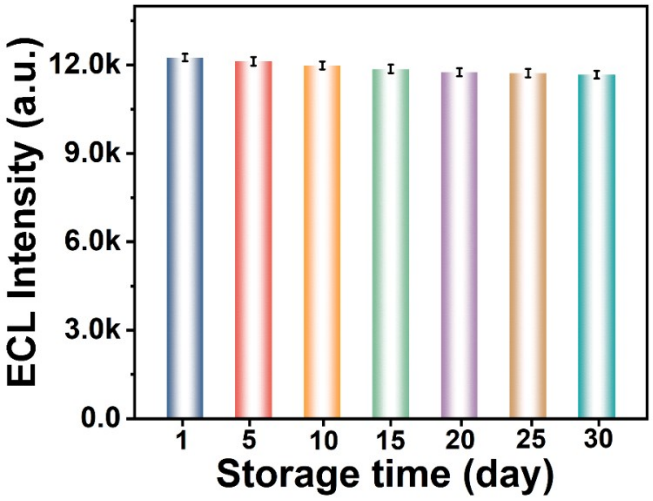

Fig. S10 Storage stability of the sensing platform with 0.1 ng mL^{-1} OTA in 0.1 M PBS (pH 7.4). Error bars in all graphs represent standard deviations in triplicated experiments.

Analytical methods	Detection range	Detection limit	References
ECL	1 pg mL^{-1} - 10 ng mL^{-1}	0.47 fg mL^{-1}	[5]
ECL	0.01 pg mL^{-1} - 10 ng mL^{-1}	3.98 fg mL^{-1}	[6]
Colorimetric	0.1 pg mL^{-1} - 10 ng mL^{-1}	12.3 fg mL^{-1}	[6]
Electrochemical	5 pg L^{-1} - 5 mg L^{-1}	2.3 pg L^{-1}	[7]
Visual mode	0.5 ng L^{-1} - 5 mg L^{-1}	0.14 ng L^{-1}	[7]
Electrochemical	1 fg mL^{-1} - 250 ng mL^{-1}	0.22 fg mL^{-1}	[8]
Colorimetric	1 fg mL^{-1} - 100 ng mL^{-1}	0.25 fg mL^{-1}	[8]
Fluorescence	0.02 μg L^{-1}- 50 μg L^{-1}	1.8 ng L^{-1}	[9]
Photoelectrochemical	3.1×10^{-5} ng mL^{-1}- 10^{2} ng mL^{-1}	0.017 pg mL^{-1}	[10]
Chemiluminescence	0.24 ng mL^{-1}- 250 ng mL^{-1}	0.08 ng mL^{-1}	[11]
Fluorescence	1 ng mL^{-1}- 100 ng mL^{-1}	0.17 ng mL^{-1}	[12]
ECL	10^{-5} ng mL^{-1} - 10^{3} ng mL^{-1}	0.13 fg mL^{-1}	This work

Table S1. Comparison of different analytical methods for OTA.

Samples	Number	Measured (ng mL^{-1})	Added (ng mL^{-1})	Founded (ng mL^{-1})	Recovery (%)	RSD (%)
corn	1	0	1	1.016	101.6	3.97
	2	0	10	9.978	99.78	2.29
	3	0	100	99.25	99.25	3.23
peanut	1	0	1	1.012	101.2	3.52
	2	0	10	9.938	99.38	3.13
	3	0	100	98.72	98.72	2.98

Table S2. Detection of OTA in real samples.

References

1.L. Wang, W.-J. Zeng, X. Yang, R. Yuan, W.-B. Liang and Y. Zhuo, Engineering Molecular Emission Centers of Carbon Dots to Boost the Electrochemiluminescence for the Detection of Cancer Cells, *Anal. Chem.*, 2023, **95**, 13897-13903.

2.Y. Wang, Y. Lang, Q. Yang and P. Wu, Breaking the Photostability and pH Limitation of Halo-Fluoresceins through Chitosan Conjugation, *Adv. Mater.*, 2023, **35**, 2210956.

3.Z. Chen, P. Chen, Y. Zhu, J. Qian, X. Huang, W. Zhang, H. Zhang, Q. Mo, Y. Lu and Y. Zhang, 2D Cobalt Oxyhydroxide Nanozymes Inhibit Inflammation by Targeting the NLRP3 Inflammasome, *Adv. Funct. Mater.*, 2023, **33**, 2214693.

4.Y. Lin, N. Lu, J. Ma, J.-H. Cheng and D.-W. Sun, High sensitive Ratiometric fluorescent Aptasensor with AIE properties for Deoxynivalenol (DON) detection, *Food Chem.*, 2024, **460**, 140550.

5.L. Song, X. Cao, Y. Yang, W. Chu, X. Zou, L. Cui and C.-Y. Zhang, Construction of a Self-Enhanced Electrochemiluminescent Sensor Based on Tandem Signal Amplification and a Self-Luminescent Lanthanide Covalent-Organic Polymer for Ochratoxin A Assay, *Anal. Chem.*, 2025, **97**, 4217-4223.

6.H. Li, Q. Cai, P. Li and G. Jie, Zero-Background Dual-Mode Closed Bipolar Electrode Electrochemiluminescence Biosensor Based on ZnCoN-C Potential Regulation for Ultrasensitive Detection of Ochratoxin A, *Anal. Chem.*, 2024, **96**, 13987-13995.

7.X. Feng, L. Ding, N. Hao and K. Wang, A Piezoelectric Nanogenerator-Driven Dual-Mode Platform for Visualization and Impedance Sensing, *Anal. Chem.*, 2024, **96**, 12553-12560.

8.Y.-L. Li, Y.-Y. Chen, F.-T. Xie, Q.-X. Li, T. Yang, Y.-H. Yang and R. Hu, Smartphone-based dual-mode aptasensor with bifunctional metal-organic frameworks as signal probes for ochratoxin A detection, *Food Chem.*, 2025, **464**, 141540.

9.C. Wang, T. Sha, J. Lu, Y. Guan and X. Geng, A Miniaturized and Highly Sensitive "Windmill" Three-Channel Fluorescence Detector for Simultaneous Detection of Various Mycotoxins, *Anal. Chem.*, 2024, **96**, 10121-10126.

10.G. Wang, L. Li, H. Zhao, H. Yang, L. Zhang, P. Zhao, K. Cui and J. Yu, Host–Guest Interaction Mediated Perovskite@Metal–Organic Framework Z-Scheme Heterojunction Enabled Paper-Based Photoelectrochemical Sensing, *Anal. Chem.*, 2024, **96**, 12165-12172.

11.L. Yu, C. Yang, S. Cheng, Q. Jiang, Y. Pang and X. Shen, Top-Down Computational Design of Molecule Recognition Peptides (MRPs) for Enzyme-Peptide Self-Assembly and Chemiluminescent Biosensing, *Anal. Chem.*, 2025, **97**, 355-364.

12.H. Wang, B. Zhao, Y. Ye, X. Qi, Y. Zhang, X. Xia, X. Wang and N. Zhou, A fluorescence and surface-enhanced Raman scattering dual-mode aptasensor for rapid and sensitive detection of ochratoxin A, *Biosens. Bioelectron.*, 2022, **207**, 114164.